Applied Surface Science 258 (2012) 3598–3603

Contents lists available at SciVerse ScienceDirect

Applied Surface Science

journal homepage: www.elsevier.com/locate/apsusc

Effect of pulse repetition rate and number of pulses in the analysis of polypropylene and high density polyethylene by nanosecond infrared laser induced breakdown spectroscopy

Flavio O. Leme[a], Quienly Godoi[a,b], Paulo H.M. Kiyataka[c], Dario Santos Jr.[d], José A.M. Agnelli[e], Francisco J. Krug[a,*]

[a] Laboratório de Química Analítica "Henrique Bergamin Filho", Centro de Energia Nuclear na Agricultura, Universidade de São Paulo, Av. Centenário 303, 13416-000 Piracicaba, SP, Brazil
[b] Departamento de Química, Universidade Federal de São Carlos, Rod. Washington Luís, km 235, 13565-905 São Carlos, SP, Brazil
[c] Centro de Tecnologia de Embalagens, Instituto de Tecnologia de Alimentos, Av. Brasil 2880, 13070-178 Campinas, SP, Brazil
[d] Departamento de Ciências Exatas e da Terra, Universidade Federal de São Paulo, Rua Prof. Artur Riedel 275, 09972-270 Diadema, SP, Brazil
[e] Departamento de Engenharia de Materiais, Universidade Federal de São Carlos, Rod. Washington Luís, km 235, 13565-905 São Carlos, SP, Brazil

ARTICLE INFO

Article history:
Received 28 July 2011
Received in revised form
25 November 2011
Accepted 25 November 2011
Available online 6 December 2011

Keywords:
LIBS
Laser induced breakdown spectroscopy
Laser pulse repetition rate
Craters characterization
High density polyethylene
Polypropylene

ABSTRACT

Pulse repetition rates and the number of laser pulses are among the most important parameters that do affect the analysis of solid materials by laser induced breakdown spectroscopy, and the knowledge of their effects is of fundamental importance for suggesting analytical strategies when dealing with laser ablation processes of polymers. In this contribution, the influence of these parameters in the ablated mass and in the features of craters was evaluated in polypropylene and high density polyethylene plates containing pigment-based $PbCrO_4$. Surface characterization and craters profile were carried out by perfilometry and scanning electron microscopy. Area, volume and profile of craters were obtained using Taylor Map software. A laser induced breakdown spectroscopy system consisted of a Q-Switched Nd:YAG laser (1064 nm, 5 ns) and an Echelle spectrometer equipped with ICCD detector were used. The evaluated operating conditions consisted of 10, 25 and 50 laser pulses at 1, 5 and 10 Hz, 250 mJ/pulse (85 J cm^{-2}), 2 μs delay time and 6 μs integration time gate. Differences in the topographical features among craters of both polymers were observed. The decrease in the repetition rate resulted in irregular craters and formation of edges, especially in polypropylene sample. The differences in the topographical features and ablated masses were attributed to the influence of the degree of crystallinity, crystalline melting temperature and glass transition temperature in the ablation process of the high density polyethylene and polypropylene. It was also observed that the intensities of chromium and lead emission signals obtained at 10 Hz were two times higher than at 5 Hz by keeping the number of laser pulses constant.

1. Introduction

LIBS has been established as an important analytical tool which allows direct analysis of solids without or with minimum sample preparation. This technique uses laser ablation for sampling and subsequent measurement of the emission intensity of UV–visible radiation from excited atoms and/or ions in laser-induced microplasma [1,2]. Laser ablation promotes the direct sampling irrespective of the form of the material. The ablation process depends on the interaction of laser pulses with the sample surface and results in crater formation in solids [3].

The potential of the LIBS for the characterization and chemical mapping of surfaces has been demonstrated [4–16]. LIBS presents the advantages of performing analysis in few seconds, allowing direct sampling from any material irrespective of its conductive status in air atmospheric pressure, simplifying the analytical sequence by minimizing and/or avoiding sample preparation steps, and presenting no limitations or minimum restrictions regarding to sample size [4,16].

In a review paper, Vadillo and Laserna emphasize that the introduction of compact and reliable solid state lasers and technological development in multidimensional intensified detectors have enabled the seeking of new analytical niches for LIBS, where their advantages could be explored. In addition to the above-mentioned advantages, the capability of LIBS for spot analysis, line scan, depth-profiling, area analysis and compositional mapping with a single instrument in the air, under atmospheric pressure, makes the technique a useful tool for surface analysis and chemical mapping in different matrices [4]. Depth profiles by LIBS analysis, for example, were demonstrated in different matrices such as brass,

* Corresponding author. Tel.: +55 19 34294648; fax: +55 19 34294774.
E-mail address: fjkrug@cena.usp.br (F.J. Krug).

0169-4332
doi:10.1016/j.apsusc.2011.11.122

steels, silicon wafers, zinc and iron foils [7,8,10,17,18].LIBS allows to perform scans in the sample surface at different depths, making the evaluation of the spacial distribution of elements possible. From the scanning information, it is possible to acquire the chemical mapping of the analytes. Chemical maps also allow to evaluate contaminants in different places of the same sample. These possibilities make the application of LIBS very interesting for quality control in the industry [4]. Several studies have assessed the application of LIBS in the chemical mapping of different sample types [6,12–15]. The possibility of performing three-dimensional multielemental chemical maps of non-flat surfaces by LIBS was demonstrated by Nicolas et al. [16].Surface characterization is another task showing the potential and versatility of LIBS. However, the application to polymers is a challenging topic considering the great number of polymers with different physical properties. The laser-sample interaction depends not only on the physical properties of the sample but on laser parameters such as wavelength, energy, and repetition rate as well. Thus, the characterization of topography, volume, diameter and depth of craters is an attractive way to understand the ablation process [19,20].

Optical microscope perfilometry is a useful tool for laser craters characterization and has been applied to craters formed in metal samples (Cu, Al, and Pb) after laser ablation with femto, pico, and nanosecond laser pulses [3].

The effects of the number of pulses, pulse repetition rate and fluence during laser ablation of poly methyl methacrylate (PMMA) were studied using a KrF @ 248 nm excimer laser at pulse repetition rate of 2 and 10 Hz [21]. In this study a perfilometer was used for craters characterization. According to the authors, the thermal effects become more pronounced when the repetition rate is high enough to significantly shorten the pulse–pulse relaxation time, or when the amount of laser pulses is large enough to produce heat accumulation. In addition, craters with smoother and less porous bottom were also observed with the increase of the pulse repetition rate and the number of pulses.

The efficiency of laser ablation of paint was investigated with nanosecond pulsed Nd:YAG @ 532 nm laser as a function of repetition rate, laser fluence and pulse duration [22]. The best ablation efficiency was obtained with the highest repetition rate. The heat accumulation with each pulse in a thermal confinement regime due to the high repetition rate allowed increases in the ablation efficiency [22].Although a large number of studies on laser ablation had been carried out, few works are related to polymers. In the analysis of organics with LIBS under atmospheric pressure, the interaction between plasma and the ambient air is much more sensitive when compared with the analysis of metallic samples due to the fact that the media to be analyzed are composed of the same elemental substances. For instance, carbon, oxygen, nitrogen, and hydrogen are omnipresent and provide the common basis of the most organic materials [23]. A detailed understanding of the laser ablation induced by the plasma is a crucial step toward the increase of LIBS application for these samples [24].

In this work, the effects of pulse repetition rate and number of pulses on the topographical features of the craters in LIBS analysis of high density polyethylene (HDPE) and polypropylene (PP) were studied by scanning electron microscopy (SEM) and perfilometry.

2. Experimental

2.1. LIBS instrumentation

Experiments were carried out with a Q-switched Nd:YAG laser (Brilliant, Quantel, France) at 1064 nm, generating 5 ns pulses of (365 ± 3) mJ in a 6 mm diameter beam with quality factor M^2 smaller than 2, at 1, 5, and 10 Hz repetition rate. The laser pulses were focused on the test sample by a convergent lens with 2.54 cm diameter and 20 cm focal length (Edmund Optics, USA). The plasma emitted radiation was collected using a fused silica lens (i.e. 80 mm focal length) and collimated into a spectrometer fiber (1.5 m, 600 μm core) matching its numerical aperture using a lens of 50 mm focal length (LLA Instruments GmbH, Germany). The optical axis of the collecting system was approximately 25° from the laser axis.

A model ESA 3000 spectrometer (LLA Instruments GmbH, Germany) equipped with echelle optics and focal length of 25 cm with aperture of 1:10 was used, which provides a 24.5 mm × 24.5 mm flat image plane. This was selected as a compromise between resolution in the wavelength range of 200–780 nm with resolving power ranging from 10,000 to 20,000. The linear dispersion per pixel ranges from 5 pm at 200 nm to 19 pm at 780 nm. The detector is an ICCD camera, comprised a Kodak KAF 1001 CCD array of 1024 × 1024 pixels full frame (24 μm × 24 μm) and a microchannel plate image intensifier of 25 mm diameter coupled to a UV-enhanced photocathode. The image signals are digitalized in dynamic range of 16 bits and further processed by a computer. The dark current of the ICCD was automatically subtracted from the measured spectral data. The instrumental parameters were defined elsewhere [25] and consisted of 18 cm lens-to-sample distance (f = 20 cm), 250 mJ per pulse (85 J cm^{-2}), 2 μs delay time and 6 μs integration time gate.

2.2. LIBS analysis

Polymer plates were produced with HDPE and PP containing 2% (w/w) of $PbCrO_4$ based pigment (Pigment Red 104; CAS Number: 12656-85-8). Polymers were weighted and mixed with pigment and the mixture was injected using a Battenfeld model 350 Plus at 200 °C and 70 bar. A 23 s injection cycle followed by 17 s cooling was used. After preparation, the densities of HDPE and PP with $PbCrO_4$ based pigment were 1.056 and 1.002 g cm^{-3}, respectively.

Test samples were obtained from each polymer plate by manually cutting parts of the sample in the form of flat disks (e.g. 3.0 cm). The selected test sample was placed in the sample holder of the ablation unit, which was assisted by a two-axis manual controlled translation stage that moved in the plane orthogonal to the laser direction. In order to displace the ambient air atmosphere from the sample surface, a laminar stream of argon was continuously fed into the sample holder assembly from below, flowing at 1.0 L min^{-1}.

LIBS spectra were collected according to the following procedure: a series of accumulated spectra was obtained after 10, 25 and 50 laser pulses per site at 1, 5 and 10 Hz repetition rate. The average of five accumulated spectra collected from 5 sites on the pellet surface was used as the representative spectrum. For each polymer, LIBS data treatment was based on three representative spectra (n = 3). ESAWIN software, NIST Atomic Database [26] and a routine developed at MATLAB® version 7.0 (MathWorks, Inc., Natick, USA) software were used for data acquisition and data treatment.

2.3. Perfilometry and scanning electron microscopy (SEM)

Topographical informations of craters were obtained with a Formtracer SV-C525 perfilometer (Taylor Hobson Precision, England). Volume, area and profile of each crater were calculated with Taylor Map software tools.

The SEM images of craters were examined by a scanning electron microscope LEO, model Stereoscan 440. The ablated surfaces were Pt-coated during 80 s using a metalizer Bal-tec, model MED 020.

3. Results and discussion

Figs. 1 and 2 show typical 3D images of craters formed on the surface of HDPE and PP. The laser fluence at the target surface for all test samples (i.e. plates) was 85 J cm^{-2}, which was defined experimentally in a previous work dealing with polymeric toys analysis [25]. The images show that width and depth of the crater increase with the number of pulses and repetition rate for both polymers. The mass of material removed during the ablation with different number of pulses and repetition rate was estimated from the crater volume calculated by Taylor Map® software. Table 1 shows the ablated masses in HDPE and PP plates after 10, 25 and 50 laser pulses with repetition rates of 1, 5 and 10 Hz. The estimated ablated masses were based on the average crater volumes at 5 different sites in the same test sample.

The perfilometric images (Figs. 1 and 2) of both polymers at 1 Hz laser repetition rate show irregular crater formation and larger variance in the mass removal when the minimum number of 10

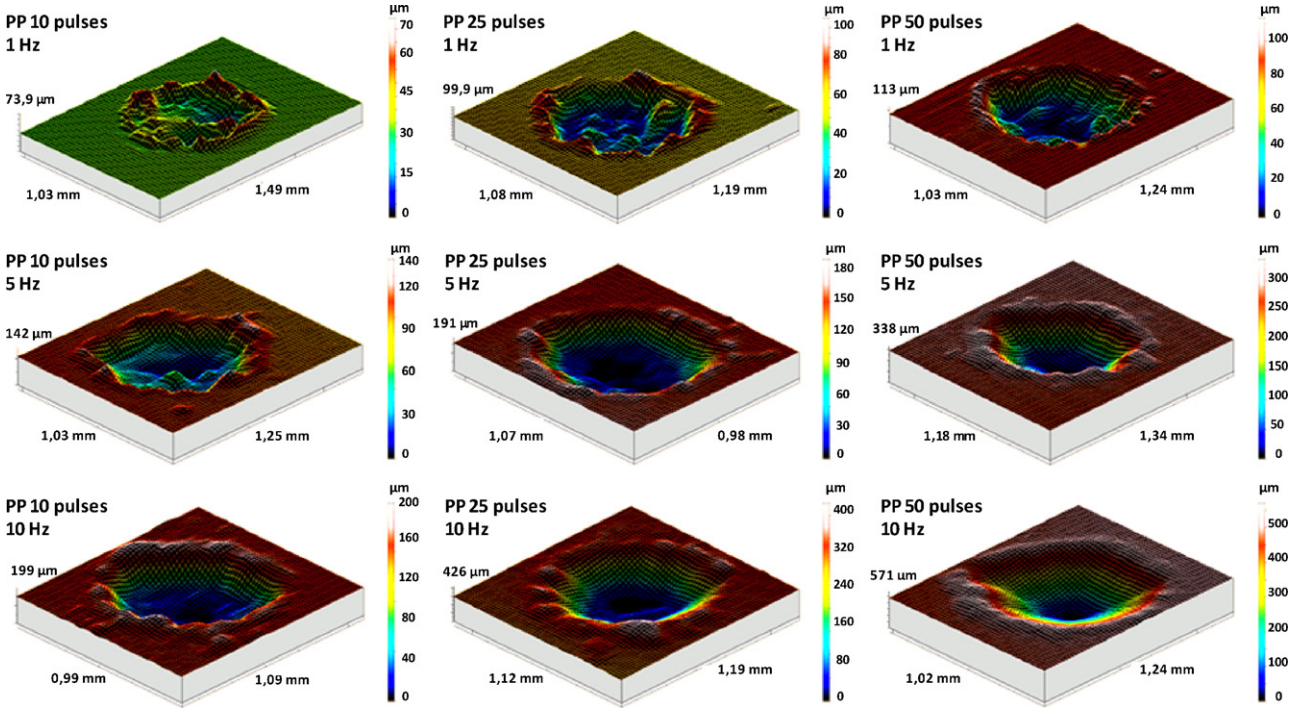

Fig. 1. Perfilometric images of craters after 10, 25 and 50 laser pulses at pulse repetititon rates of 1, 5 and 10 Hz in PP.

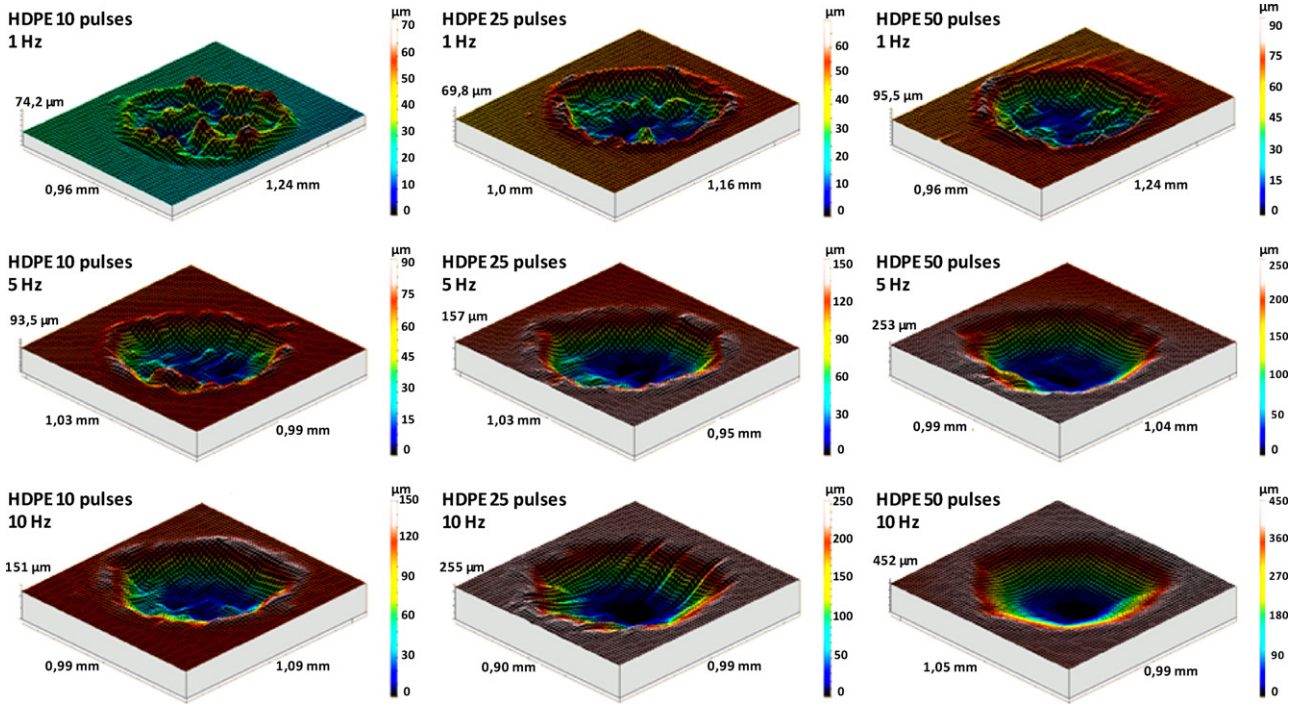

Fig. 2. Perfilometric images of craters after 10, 25 and 50 laser pulses at pulse repetititon rates of 1, 5 and 10 Hz in HDPE.

Table 1
Ablated masses in HDPE and PP plates after 10, 25 and 50 laser pulses at 1, 5 and 10 Hz repetition rates. Uncertainties are represented by ±1 estimated standard deviation (n = 5 craters).

Laser pulses	Ablated mass (μg)	
	HDPE	PP
	1 Hz	
50	15 ± 2	14 ± 2
25	8 ± 2	11 ± 2
10	3 ± 1	3 ± 1
	5 Hz	
50	46 ± 4	47 ± 7
25	23 ± 2	32 ± 2
10	9 ± 2	16 ± 3
	10 Hz	
50	88 ± 6	80 ± 8
25	43 ± 5	61 ± 5
10	22 ± 3	33 ± 4

laser pulses was applied. For 25 and 50 consecutive laser pulses the resulting craters presented more uniform geometry. Small edges around the crater for both polymers can be observed, which were probably due to the thermal effects caused by the relatively large time interval between pulses (100–1000 ms), which results in cooling. Consequently, the ablation surface becomes quite irregular after the end of the ablation process. Irregular and porous ablated surface was also observed in PMMA [21]. According to the authors, these effects were related to thermal effects during the plasma formation and affected by the laser wavelength, laser pulse repetition rate and the number of laser pulses.

In the present case, high coefficients of variation (>35%) in the calculated ablated masses were observed for craters formed with 10 laser pulses at 1 Hz in both HDPE and PP plates. When craters were formed by applying 25 and 50 pulses at the same repetition rate, this uncertainty decreased to 20%, which was expected due to a better sampling process.

On the other hand, craters were much more uniform by applying 10, 25 or 50 laser pulses at 5 and 10 Hz and the coefficients of variation of mass removal were between 18% and 5%, respectively. The small edges around the craters were observed in HDPE samples by applying 10 and 25 laser pulses at 5 Hz and 10 laser pulses at 10 Hz. In the PP plates, edges were observed in the surroundings of all craters.

The ablated masses with repetition rates of 5 and 10 Hz (Table 1) show a considerable difference between the HDPE and PP after 10 and 25 laser pulses. The mass removal from PP was considerably larger than the one removed from HDPE. For 50 laser pulses, non-significant differences between the ablated masses from both polymers were observed. The formation of edges and differences in crater's geometry in function of polymer composition were also observed by Godoi et al. [25].

Thermal effects of the ablation process were more pronounced for PP than HDPE, and more uniform craters being observed in HDPE (Fig. 3). The perfilometries of the ablated sites in both PP and HDPE plates, obtained after 50 laser pulses at 10 Hz, showed that craters' depth were approximately 420 and 550 μm, respectively.

Polymer laser ablation involves photothermal and/or photochemical processes, depending on the nature of the polymers and the laser parameters [27–29]. According to Pham et al. [30] the

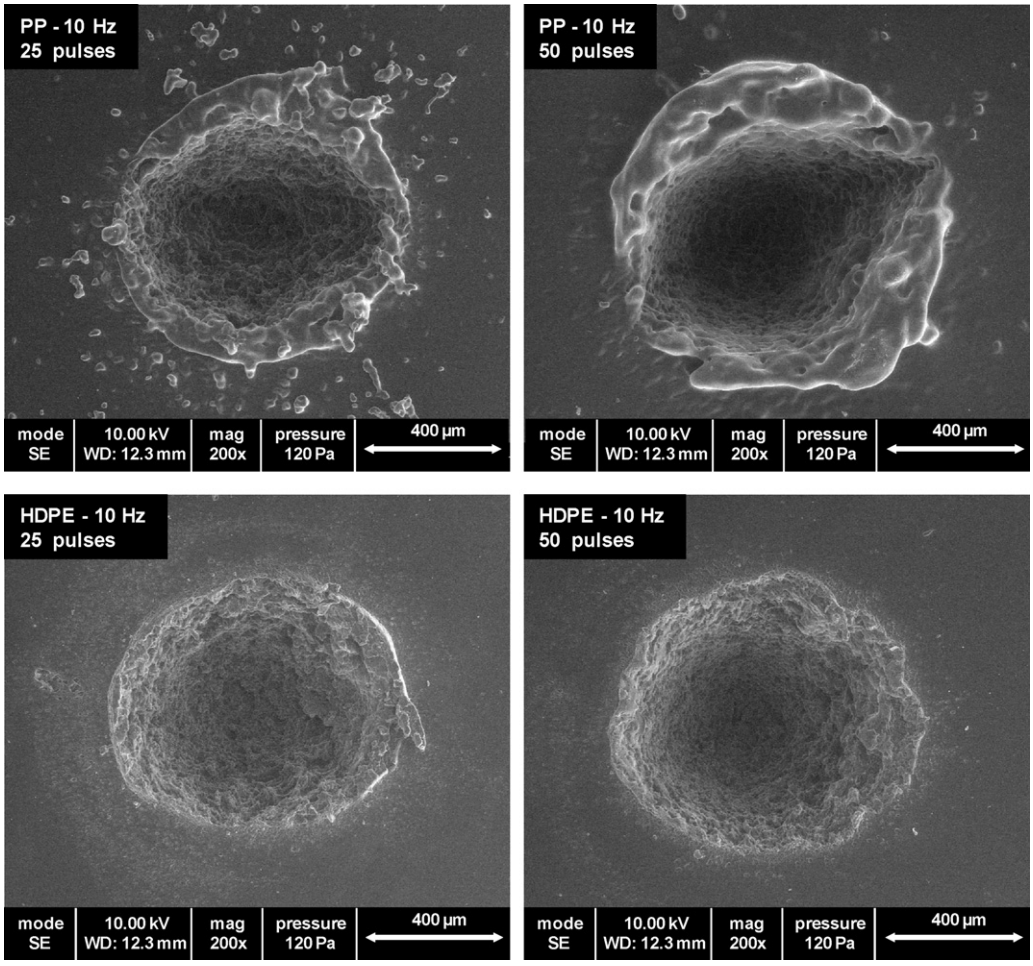

Fig. 3. SEM images of the craters formed in PP and HDPE plates after 25 and 50 laser pulses at 10 Hz.

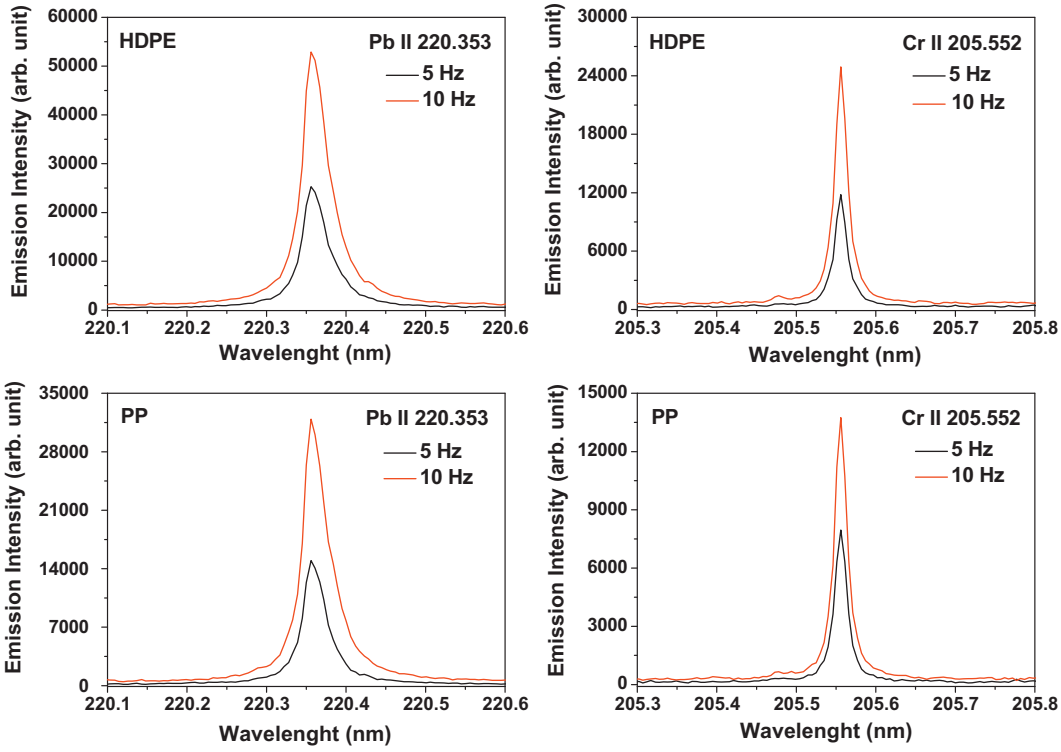

Fig. 4. Pb II 220.353 and Cr II 205.552 nm LIBS emission lines signals from HDPE containing $2000 \pm 40\,mg\,kg^{-1}$ Cr and $6980 \pm 200\,mg\,kg^{-1}$ Pb, and from PP with $1420 \pm 20\,mg\,kg^{-1}$ Cr and $5650 \pm 120\,mg\,kg^{-1}$ Pb after 25 laser pulses at 5 and 10 Hz.

photothermal process involves the absorption of photons, followed by release of these photons into the polymer matrix. This process induces a rapid temperature rise in the bulk material leading to the thermal decomposition of the polymer. According to the authors, if the vibrational energy attains a particular fluence threshold, the chemical bonds in the polymer will break, resulting in a phenomenon known as photofragmentation. These fragments typically occupy a larger volume compared to the surrounding material and lead to the forwarded ejection of ablated material.

In the present study, only the photothermal process takes place because the experiments were carried out with laser operating in the infrared (1064 nm), which is in contrast with the photochemical process that promotes breaking of chemical bonds with ns UV pulses, as commented elsewhere [30]. Therefore, the main properties that may influence the ablation process are degree of crystallinity, crystalline melting temperature (T_m) and glass transition temperature (T_g).

Crystallinity in polymers refers to an arrangement of molecules that denote uniformity and compactness of the molecular chains and can be attributed to the formation of solid crystals having a definite geometric form [31]. Thus, the crystalline region is the part of the polymer that has these features. In contrast, the amorphous region is the part of the polymer that has a random structure and, consequently, does not have a molecular order defined. Degree of crystallinity is defined as the ratio of the crystalline region and the amorphous region of the polymer.

The T_m is the temperature at which the crystalline region of the polymer disintegrates and merges. In this temperature, both the liquid and the solid phases have the same Gibbs free energy and the polymeric chain become liquid without established order [32,33]. The T_g is the approximate midpoint of the temperature range over which the primary glass transition takes place. T_g is related to the stiffness of the molecular segments, degree of cross-linking, entanglement and crystallization kinetics [31,32].

PP and HDPE have a similar structure and the only difference is that PP's chemical structure has a CH_3 group linked to one of the carbons of the monomer. PP and HDPE have linear structures but, due to the presence of the CH_3 group, PP has a helical configuration with angles of 120° among the methyl groups. The presence of the CH_3 group is responsible for the differences in the properties of both polymers, mainly density, degree of crystallinity, T_m, and T_g.

PP has a lower density than HDPE due to the steric effect caused by CH_3 groups, which make the packing of macromolecules less effective for PP. This fact is also related to differences in T_m, T_g and the degree of crystallinity of both polymers. For PP, T_m is between 165 and 175 °C and T_g between 4 and 12 °C. For HDPE, T_m is 135° C and T_g is −120° C. The degree of crystallinity varies between 50% and 70% for PP and up to 95% for HDPE [34]. The degree of crystallinity can be determined by several experimental techniques. The most commonly used are X-ray diffraction, differential scanning calorimetry, density measurements and infrared spectroscopy. However, imperfections in the crystalline structure are not easily distinguished from the amorphous phase and these techniques may be affected to a different extent by imperfections [35]. Disagreements among results of quantitative measurements of crystallinity are frequently encountered [35], and it is common to find values between 50% and 70% for PP and from 80% up to 95% for HDPE [34].

The results found herein suggest that the differences in the degree of crystallinity, T_m and T_g are crucial in the ablation process of PP and HDPE. As aforementioned, the interaction of ns laser pulses at 1064 nm with the polymer results in the absorption of photons, generating a fast increase in local temperature. The molecules acquire thermal energy sufficient to move the chains and, consequently, to break the chemical bonds resulting in photofragmentation. Due to the lower degree of crystallinity and higher T_g of the PP compared to HDPE, its amorphous region is considerably higher. Consequently, the polymeric chains acquire mobility more easily, and the chemical bonds of PP are more easily broken than those of HDPE. After the PP chemical bonds are broken a fraction of the removed fragments is vaporized and consumed in the plasma. Therefore, the mass removal of PP after 10 and 25 pulses

at 5 and 10 Hz is higher than of the HDPE. When 50 laser pulses are applied, the difference in the mass removal is minimized. At 1 Hz no differences in the mass removal were observed, most probably due to the large time interval between pulses.

The formation of edges more pronounced around PP craters, suggest that occur a higher effect of the T_m in the ablation process of PP compared to HDPE. As the temperature in the borders of the plasma is relatively low, and the PP has higher T_m compared with HDPE, the formation of pronounced edges in PP plates occurs because the temperature of the borders of plasma is not enough for complete vaporization of the material.Fig. 4 shows the emission peak profiles for Cr and Pb obtained by LIBS in HDPE and PP after 25 laser pulses at 5 and 10 Hz. It can be observed that the intensities obtained at laser repetition rate of 10 Hz are two times higher than those at 5 Hz. These results are consistent with the mass removal during the ablation process, as shown in Table 1.

4. Conclusions

Perfilometry and SEM are useful tools for laser craters characterization. The images allow features evaluation and the mass removal of HDPE and PP can be calculated through data obtained by perfilometry. Small edges around the craters and high coefficients of variation in the mass removal were observed at 1 Hz repetition rate in both polymer plates. For 25 and 50 laser pulses remarkable improvements in either the geometry of craters as well as in the coefficients of variation of the ablated masses were observed. HDPE and PP showed significant differences in mass removal with 10 and 25 laser pulses at 5 and 10 Hz repetition rate, but with 50 pulses similar results were obtained.

Results indicate that the main properties that influence the ablation process in polymers are the degree of crystallinity, the T_m and the T_g. Due the remarkable differences between these properties for both polymers, the thermal effects were more pronounced in PP and, consequently, the perfilometric images of the ablated sites showed craters with pronounced edges. The higher degree of crystallinity and the lower T_m and T_g are the possible reasons to explain why the formation of small edges were not observed in craters formed in HDPE plates when 25 and 50 laser pulses at 10 Hz were applied.

Acknowledgements

Authors are thankful to Conselho Nacional de Desenvolvimento Científico e Tecnológico (CNPq 140879/2008-0 and 305913/2009-3) and Fundação de Amparo à Pesquisa do Estado de São Paulo (FAPESP 07/01052-3) for grants and financial support. Authors are also grateful to Prof. Younnes Messaddeq (IQ-UNESP) for helping in perfilometric analysis, to Prof. Jez W. B. Braga (IQ-UNB) for the Matlab routine and to Liz Zanchetta (EP-USP) for helping with SEM analysis.

References

[1] A.W. Miziolek, V. Palleschi, I. Schechter, Laser-Induced Breakdown Spectroscopy, first ed., Cambridge University Press, Cambridge, 2006.
[2] J.P. Singh, S.N. Thakur, Laser-Induced Breakdown Spectroscopy, first ed., Elsevier, Amsterdam, 2007.
[3] A. Semerok, B. Salle, J.F. Wagner, G. Petite, Femtosecond, picosecond, and nanosecond laser microablation: laser plasma and crater investigation, Laser Part. Beams 20 (2002) 67–72.
[4] J.M. Vadillo, J.J. Laserna, Laser-induced plasma spectrometry: truly a surface analytical tool, Spectrochim. Acta B 59 (2004) 147–161.
[5] J.M. Vadillo, I. Vadillo, F. Carrasco, J.J. Laserna, Spatial distribution profiles of magnesium and strontium in speleothems using laser-induced breakdown spectrometry, Fresenius J. Anal. Chem. 361 (1998) 119–123.
[6] H. Wiggenhauser, D. Schaurich, G. Wilsch, LIBS for non-destructive testing of element distributions on surfaces, NDT & E Int. 31 (1998) 307–313.
[7] J.M. Vadillo, J.J. Laserna, Depth-resolved analysis of multilayered samples by laser-induced breakdown spectrometry, J. Anal. Atom. Spectrom. 12 (1997) 859–862.
[8] J.M. Vadillo, C.C. Garcia, S. Palanco, J.J. Laserna, Nanometric range depth-resolved analysis of coated-steels using laser-induced breakdown spectrometry with a 308 nm collimated beam, J. Anal. Atom. Spectrom. 13 (1998) 793–797.
[9] L. St-Onge, M. Sabsabi, Towards quantitative depth-profile analysis using laser-induced plasma spectroscopy: investigation of galvannealed coatings on steel, Spectrochim. Acta B 55 (2000) 299–308.
[10] D.R. Anderson, C.W. McLeod, T. English, A.T. Smith, Depth profile studies using laser-induced plasma emission spectrometry, Appl. Spectrosc. 49 (1995) 691–701.
[11] J.M. Vadillo, S. Palanco, M.D. Romero, J.J. Laserna, Applications of laser-induced breakdown spectrometry (LIBS) in surface analysis, Fresenius J. Anal. Chem. 355 (1996) 909–912.
[12] T. Kim, C.T. Lin, Y. Yoon, Compositional mapping by laser-induced breakdown spectroscopy, J. Phys. Chem. B 102 (1998) 4284–4287.
[13] P. Lucena, J.M. Vadillo, J.J. Laserna, Mapping of platinum group metals in automotive exhaust three-way catalysts using laser-induced breakdown spectrometry, Anal. Chem. 71 (1999) 4385–4391.
[14] P. Lucena, J.J. Laserna, Three-dimensional distribution analysis of platinum, palladium and rhodium in auto catalytic converters using imaging-mode laser-induced breakdown spectrometry, Spectrochim. Acta B 56 (2001) 177–185.
[15] P. Lucena, J.M. Vadillo, J.J. Laserna, Compositional mapping of poisoning elements in automobile three-way catalytic converters by using laser-induced breakdown spectrometry, Appl. Spectrosc. 55 (2001) 267–272.
[16] G. Nicolas, M.P. Mateo, V. Pinon, 3D chemical maps of non-flat surfaces by laser-induced breakdown spectroscopy, J. Anal. Atom. Spectrom. 22 (2007) 1244–1249.
[17] M. Milan, P. Lucena, L.M. Cabalin, J.J. Laserna, Depth profiling of phosphorus in photonic-grade silicon using laser-induced breakdown spectrometry, Appl. Spectrosc. 52 (1998) 444–448.
[18] J.M. Vadillo, J.M.F. Romero, C. Rodriguez, J.J. Laserna, Depth-resolved analysis by laser-induced breakdown spectrometry at reduced pressure, Surf. Interface Anal. 26 (1998) 995–1000.
[19] B. Salle, C. Chaleard, V. Detalle, J.L. Lacour, P. Mauchien, C. Nouvellon, A. Semerok, Laser ablation efficiency of metal samples with UV laser nanosecond pulses, Appl. Surf. Sci. 138 (1999) 302–305.
[20] A. Semerok, C. Chaleard, V. Detalle, J.L. Lacour, P. Mauchien, P. Meynadier, C. Nouvellon, B. Salle, P. Palianov, M. Perdrix, G. Petite, Experimental investigations of laser ablation efficiency of pure metals with femto, pico and nanosecond pulses, Appl. Surf. Sci. 138 (1999) 311–314.
[21] Z.Q. Liu, Y. Feng, X.S. Yi, Coupling effects of the number of pulses, pulse repetition rate and fluence during laser PMMA ablation, Appl. Surf. Sci. 165 (2000) 303–308.
[22] F. Brygo, C. Dutouquet, F. Le Guern, R. Oltra, A. Semerok, J.M. Weulersse, Laser fluence, repetition rate and pulse duration effects on paint ablation, Appl. Surf. Sci. 252 (2006) 2131–2138.
[23] M. Baudelet, M. Boueri, J. Yu, S.S. Mao, V. Piscitelli, X. Mao, R.E. Russo, Time-resolved ultraviolet laser-induced breakdown spectroscopy for organic material analysis, Spectrochim. Acta B 62 (2007) 1329–1334.
[24] M. Boueri, M. Baudelet, J. Yu, X.L. Mao, S.S. Mao, R. Russo, Early stage expansion and time-resolved spectral emission of laser-induced plasma from polymer, Appl. Surf. Sci. 255 (2009) 9566–9571.
[25] Q. Godoi, D. Santos, L.C. Nunes, F.O. Leme, I.A. Rufini, J.A.M. Agnelli, L.C. Trevizan, F.J. Krug, Preliminary studies of laser-induced breakdown spectrometry for the determination of Ba, Cd, Cr and Pb in toys, Spectrochim. Acta B 64 (2009) 573–581.
[26] NIST Atomic Spectra Database (National Institute of Standards and Technology), http://physics.nist.gov/PhysRefData/ASD/lines_form.html (accessed April 2011).
[27] H. Sato, S. Nishio, Polymer laser photochemistry, ablation, reconstruction, and polymerization, J. Photochem. Photobiol. C 2 (2001) 139–152.
[28] A.A. Serafetinides, M.I. Makropoulou, C.D. Skordoulis, A.K. Kar, Ultrashort pulsed laser ablation of polymers, Appl. Surf. Sci. 180 (2001) 42–56.
[29] C. Hahn, T. Lippert, A. Wokaun, Comparison of the ablation behavior of polymer films in the IR and UV with nanosecond and picosecond pulses, J. Phys. Chem. B 103 (1999) 1287–1294.
[30] D. Pham, L. Tonge, J. Cao, J. Wright, M. Papiernik, E. Harvey, D. Nicolau, Effects of polymer properties on laser ablation behaviour, Smart Mater. Struct. 11 (2002) 668–674.
[31] L.H. Sperling, Introduction to Physical Polymer Science, fourth ed., John Wiley & Sons, Hoboken, 2006.
[32] C.A. Harper, E.M. Petrie, Plastics Materials and Processes: A Concise Encyclopedia, first ed., John Wiley & Sons, Hoboken, 2003.
[33] D.I. Bower, An Introduction to Polymer Physics, first ed., Cambridge University Press, Cambridge, 2002.
[34] E.B. Mano, L.C. Mendes, Introdução a polímeros, second ed., Editora Edgard Blücher Ltda, São Paulo, 1999.
[35] IUPAC, Compendium of Chemical Terminology (The Gold Book). Compiled by A.D. McNaught, A. Wilkinson, second ed., Blackwell Scientific Publications, Oxford, 1997, XML on-line corrected version: http://goldbook.iupac.org (2006).